Chalmers Publication Library

CHALMERS

Copyright Notice

©2014 IEEE. Personal use of this material is permitted. However, permission to reprint/republish this material for advertising or promotional purposes or for creating new collective works for resale or redistribution to servers or lists, or to reuse any copyrighted component of this work in other works must be obtained from the IEEE.

This document was downloaded from Chalmers Publication Library (http://publications.lib.chalmers.se/), where it is available in accordance with the IEEE PSPB Operations Manual, amended 19 Nov. 2010, Sec. 8.1.9 (http://www.ieee.org/documents/opsmanual.pdf)

(Article begins on next page)

I/Q Imbalance in Two-Way AF Relaying: Power Allocation and Performance Analysis

Jingya Li[†], Michail Matthaiou[⋆†], and Tommy Svensson[†]
[†]Department of Signals and Systems, Chalmers University of Technology, Gothenburg, Sweden
[⋆]School of Electronics, Electrical Engineering and Computer Science, Queen's University Belfast, Belfast, U.K.
Email: jingya.li@chalmers.se, tommy.svensson@chalmers.se, m.matthaiou@qub.ac.uk

***Abstract*—We investigate the performance of dual-hop two-way amplify-and-forward (AF) relaying in the presence of in-phase and quadrature-phase imbalance (IQI) at the relay node. In particular, the effective signal-to-interference-plus-noise ratio (SINR) at both sources is derived. These SINRs are used to design an instantaneous power allocation scheme, which maximizes the minimum SINR of the two sources under a total transmit power constraint. The solution to this optimization problem is analytically determined and used to evaluate the outage probability (OP) of the considered two-way AF relaying system. Both analytical and numerical results show that IQI can create fundamental performance limits on two-way relaying, which cannot be avoided by simply improving the channel conditions.**

I. Introduction

Relaying-assisted transmission is considered as one of the key technologies for future wireless networks thanks to its capability of improving the system reliability, extending network coverage and ensuring quality of service [1]. The amplify-and-forward (AF) and decode-and-forward are two popular relaying protocols. Recall that the former has lower implementation complexity, since it only amplifies the received signal, without performing any decoding. In this paper, we focus on half-duplex two-way AF relaying, which allows two sources to exchange data through a relay simultaneously within two phases. Thus, it can achieve higher spectral efficiency compared to standard one-way relaying [2], [3].

Most works in the area of relaying assume that the transceiver hardware of the relay is perfect [2]–[5]. However, in practice, due to the limited accuracy of the analog hardware and the up/down conversion operations at the relay, relaying systems are intimately affected by hardware impairments, e.g., phase noise, power amplifier nonlinearities, and in-phase and quadrature-phase imbalance (IQI). In this paper, we focus on the impact of IQI, which refers to the phase and amplitude mismatch between the in-phase (I) and quadrature (Q) signals at the transmitter (TX) and receiver (RX) sides. Such imbalance creates an additional image-signal, leading to significant performance loss especially in high-rate systems [6]. Since the hardware of the low-cost relay nodes is most likely to be of poor quality, relays are more prone to IQI.

This work was supported in part by the Swedish Governmental Agency for Innovation Systems (VINNOVA) within the VINN Excellence Center Chase, and the Swedish Research Council VR under the project 621-2009-4555 Dynamic Multipoint Wireless Transmission.

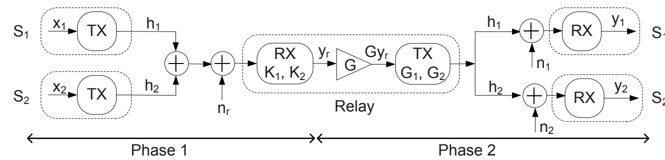

Fig. 1. Dual-hop two-way AF relaying with IQI at the relay node.

Despite the importance of IQI for relaying systems, there are only a few relevant works reported in the literature. In particular, the IQI effects on one-way AF relaying were investigated in [7], [8], where novel digital baseband compensation algorithms were proposed. In [9], analytical expressions for the OP and ergodic capacity were derived for one-way AF relaying in the presence of IQI at the relay node. Most recently, [10] elaborated on the impact of IQI on two-way AF relaying. In contrast to this paper, the authors in [10] did not consider IQI effects at the relay node and all analytical results were limited to Rayleigh fading channels. Most importantly, [10] did not work out any power allocation policy to mitigate the impact of IQI.

Motivated by the above discussion, we hereafter characterize the performance of dual-hop two-way AF relaying in the presence of IQI at the relay. First, we obtain expressions for the end-to-end SINRs at both sources. Then, an instantaneous power allocation scheme is formulated to maximize the minimum SINR, thus, improving the system reliability. With the closed-form optimal power allocation solution in hand, lower bounds on the OP are derived over independent, non-identically distributed Nakagami-m fading channels. Both analytical and numerical results show that IQI can create fundamental performance limits on two-way relaying, even with optimal power allocation. More specifically, when the target SINR value is above the inverse of the joint image-leakage ratio, as defined in Section II, the system will always be in outage. This cannot be avoided by simply improving the channel conditions, or increasing the transmit power.

II. System and Signal Model

We consider a two-way AF relaying system where two source nodes, S_1 and S_2, communicate with each other through a single relay node. All nodes are equipped with a single antenna, and transmission at all nodes is constrained to the half-duplex mode, i.e., no node can transmit and receive at the same time. The data transmission is carried out in two phases, as depicted in Fig. 1. In phase 1, S_1 and S_2 simultaneously transmit their information to the relay node. In phase 2, the relay amplifies the received signal and broadcasts it to both sources. The RF front-ends of the source and the destination are assumed to be perfect. In this paper, we focus on the impact of the IQI at the relay node, since it normally deploys lower-quality hardware.

A. IQI Model

In general, IQI refers to as the phase and amplitude imbalance between the I and Q signal paths at the transceivers. Here, we consider an asymmetrical IQI model, where the I branch is assumed to be ideal and the errors are modeled in the Q branch [6], [11]. In the case of TX IQI, the baseband representation of the up-converted TX signal can be given as

$$\hat{x} = G_1 x + G_2^* x^* \tag{1}$$

where x is the baseband TX signal under perfect TX I/Q matching. In turn, G_1, G_2 are given by

$$G_1 \triangleq \left(1 + g_T e^{j\phi_T}\right)/2 \text{ and } G_2 \triangleq \left(1 - g_T e^{-j\phi_T}\right)/2 \tag{2}$$

where g_T and ϕ_T model the TX amplitude and phase mismatch, respectively. Regarding the RX IQI, the down-conversion of the RF RX signal is given by

$$\hat{y} = K_1 y + K_2 y^* \tag{3}$$

where y denotes the down-converted baseband RX signal under perfect RX I/Q matching. The coefficients K_1 and K_2 are given by

$$K_1 \triangleq \left(1 + g_R e^{-j\phi_R}\right)/2 \text{ and } K_2 \triangleq \left(1 - g_R e^{j\phi_R}\right)/2 \tag{4}$$

where g_R and ϕ_R denote the RX amplitude and phase mismatch, respectively. The x^* and y^* terms in (1) and (3) are often referred to as the mirror signals introduced by IQI [6]. It is noted that for perfect I/Q matching, these imbalance parameters reduce to $g_T = g_R = 1$ and $\phi_T = \phi_R = 0$; thus, in this case, we will have $G_1 = K_1 = 1$ and $G_2 = K_2 = 0$.

B. End-to-end SNR

Let h_i denote the channel coefficient for the S_i-to-relay link for $i = 1, 2$. The amplitudes $g_1 \triangleq |h_1|$ and $g_2 \triangleq |h_2|$ are modeled as independent, non-identical Nakagami-m random variables with fading parameters $m_i \geq 0.5$, and average powers $\Omega_i = \mathbb{E}\left\{|h_i|^2\right\}$ for $i = 1, 2$. Here, the operator $\mathbb{E}\{\cdot\}$ stands for expectation. The complex Gaussian receiver noises at S_1, S_2, and the relay are denoted by $n_1 \sim \mathcal{CN}(0, N_1)$, $n_2 \sim \mathcal{CN}(0, N_2)$, and $n_r \sim \mathcal{CN}(0, N_r)$, respectively. For simplicity, it is assumed that all noise powers are $N_1 = N_2 = N_r = 1$. We will now use the relationships (1) and (3) to derive the end-to-end SINR for each source, considering the two-phase, two-way AF relaying protocol. We assume that the channels between the sources and the relay are reciprocal, and remain constant during these two phases; the instantaneous channel realizations of h_1 and h_2 are known at all nodes.

In phase 1, S_1 and S_2 simultaneously transmit their information to the relay node. Under RX I/Q mismatch, the baseband RX signal after down-conversion at the relay node, y_r, can be expressed as

$$y_r = K_1 (h_1 x_1 + h_2 x_2 + n_r) + K_2 (h_1 x_1 + h_2 x_2 + n_r)^* \tag{5}$$

where $x_1, x_2 \in \mathbb{C}$ are the transmitted signals from the S_1 and S_2, with average transmit power $\mathbb{E}\left\{|x_1|^2\right\} = P_1$ and $\mathbb{E}\left\{|x_2|^2\right\} = P_2$ respectively. In phase 2, the relay node amplifies the received signal at baseband with an amplification factor $\mathtt{G}$, up-converts it to RF, and then broadcasts it to both sources. With TX IQI at the relay, the baseband RX signal at S_i is given by

$$y_i = h_i \left(G_i (\mathtt{G} y_r) + G_j^* (\mathtt{G} y_r)^*\right) + n_i \tag{6}$$

where $j = \frac{2}{i}$ with $i = 1, 2$. Substituting (5) into (6), we can write the received signals at S_i as

$$\begin{aligned} y_i = {} & \mathtt{G} A h_i^2 x_i + \mathtt{G} B |h_i|^2 x_i^* + \mathtt{G} A h_i h_j x_j + \mathtt{G} B h_i h_j^* x_j^* \\ & + \mathtt{G} A h_i n_r + \mathtt{G} B h_i n_r^* + n_i \end{aligned} \tag{7}$$

where

$$A \triangleq G_1 K_1 + G_2^* K_2^* \text{ and } B \triangleq G_1 K_2 + G_2^* K_1^*. \tag{8}$$

Since the relay node has perfect instantaneous knowledge of the fading channels h_1 and h_2, the variable amplification factor $\mathtt{G}$ can be selected as

$$\mathtt{G} = \sqrt{\frac{P_r}{D(\rho_1 P_1 + \rho_2 P_2 + 1)}} \tag{9}$$

where P_r is the power of the transmitted signal at the output of the relay node. Also, $\rho_i \triangleq |h_i|^2$ for $i = 1, 2$, and

$$D \triangleq \left(|G_1|^2 + |G_2|^2\right)\left(|K_1|^2 + |K_2|^2\right). \tag{10}$$

The IQI parameters (A, B and D) and the gain factor $\mathtt{G}$ are broadcasted from the relay to both sources. Hence, each source can cancel the corresponding self-interference terms, i.e., $\mathtt{G} A h_i^2 x_i + \mathtt{G} B |h_i|^2 x_i^*$ for S_i, from which we get[1]

$$\tilde{y}_i = \mathtt{G} A h_i h_j x_j + \mathtt{G} B h_i h_j^* x_j^* + \mathtt{G} A h_i n_r + \mathtt{G} B h_i n_r^* + n_i. \tag{11}$$

Thus, the received SINR at S_i can be obtained as

$$\gamma_i = \frac{\rho_i \rho_j P_j}{\kappa \rho_i \rho_j P_j + (1+\kappa)\rho_i + \frac{1}{|A|^2 \mathtt{G}^2}} \tag{12}$$

where the ratio $\kappa \triangleq |B|^2 / |A|^2$ is referred to as the *joint image-leakage ratio* of the considered relaying system [9], [12], [13]. Note that for the case of perfect I/Q matching at the relay node, we have $A = 1$, $B = 0$ and $\kappa = 0$.

[1]Note that with knowledge of the IQI parameters (A, B and D) and the fading channels h_1 and h_2, each source node S_i can also perform standard IQI compensation by augmenting the signal $\tilde{y}_i$ with its conjugate. Power allocation with IQI compensation will be considered in the journal version of this paper.

Utilizing the general SINR expressions in (12), in the following, we study an instantaneous power allocation problem. In order to enhance the system reliability, the transmit powers are optimized to maximize the minimum SINR of the two sources for each instantaneous channel realization.

III. Optimal Power Allocation

We consider an instantaneous power allocation problem, which maximizes the minimum SINR of the two sources. It is assumed that the system has a maximum total power constraint, $P_{\max}$. From (9), the transmit power from the relay node, P_r, can be written as $P_r = \mathtt{G}^2 D(\rho_1 P_1 + \rho_2 P_2 + 1)$. Therefore, the total transmit power, P_{tot}, can be calculated as

$$P_{\text{tot}} = P_1 + P_2 + \mathtt{G}^2 D(\rho_1 P_1 + \rho_2 P_2 + 1). \quad (13)$$

For each instantaneous channel realization, the optimization problem can then be formulated as

$$\begin{aligned} &\max_{P_1, P_2, \mathtt{G}^2} \min(\gamma_1, \gamma_2) \\ &\quad \text{s.t. } P_1 + P_2 + \mathtt{G}^2 D(\rho_1 P_1 + \rho_2 P_2 + 1) \le P_{\text{max}}. \end{aligned} \quad (14)$$

From (12), we see that γ_i for $i = 1, 2$ are non-decreasing functions with respect to P_1, P_2 and $\mathtt{G}^2$. Thus, the minimum SINR is maximized when the inequality constraint in (14) is satisfied with equality. Moreover, similar to [5], we can show that $\gamma_1 = \gamma_2$ at the optimum. Hence, the power allocation problem (14) is equivalent to

$$\begin{aligned} &\max_{P_1, P_2, \mathtt{G}^2} \gamma_1 \\ &\quad \text{s.t. } P_1 + P_2 + \mathtt{G}^2 D(\rho_1 P_1 + \rho_2 P_2 + 1) = P_{\text{max}}, \gamma_1 = \gamma_2. \end{aligned} \quad (15)$$

Plugging the SINR expression (12) into the two equality constraints in (15), we have

$$P_1 = P_2 \frac{1 + \mathtt{G}^2 C \rho_2}{1 + \mathtt{G}^2 C \rho_1} \quad (16)$$

$$P_2 = \frac{(P_{\max} - \mathtt{G}^2 D)(1 + \mathtt{G}^2 C \rho_1)}{(1 + \mathtt{G}^2 C \rho_1)(1 + \mathtt{G}^2 D \rho_2) + (1 + \mathtt{G}^2 C \rho_2)(1 + \mathtt{G}^2 D \rho_1)} \quad (17)$$

where $C \triangleq |A|^2 + |B|^2$. Then, (15) can be reformulated as

$$\max_{\mathtt{G}^2} \frac{|A|^2 \mathcal{J}}{|B|^2 \mathcal{J} + 1} \quad (18)$$

where

$$\mathcal{J} \triangleq \frac{(P_{\max} - \mathtt{G}^2 D)\, \mathtt{G}^2}{(1 + \mathtt{G}^2 C \rho_1)(1 + \mathtt{G}^2 D \rho_2) + (1 + \mathtt{G}^2 C \rho_2)(1 + \mathtt{G}^2 D \rho_1)}.$$

Based on the fact that $f(x) = \frac{ax}{bx+1}$ is monotonically increasing in x, for $a, b > 0$, the problem (18) can be simplified to $\max_{\mathtt{G}^2} \mathcal{J}$. By calculating the first derivative of $\mathcal{J}$ with respect to $\mathtt{G}^2$ and setting it to zero, the optimal $\mathtt{G}^2$ can be derived as

$$\mathtt{G}^2_{\text{opt}} = \frac{P_{\max}}{D(1 + \mathcal{K})} \quad (19)$$

where $\alpha \triangleq C/D$, and

$$\mathcal{K} \triangleq \sqrt{1 + \frac{(\alpha + 1)}{2}(\rho_1 + \rho_2) P_{\max} + \alpha \rho_1 \rho_2 P_{\max}^2}. \quad (20)$$

Substituting (19) into (16) and (17), the optimal P_1, P_2 and P_r can be obtained as

$$P_{1,\text{opt}} = \frac{\mathcal{K}(\mathcal{K} + 1 + \alpha \rho_2 P_{\max})}{\mathcal{I}} P_{\max} \quad (21)$$

$$P_{2,\text{opt}} = \frac{\mathcal{K}(\mathcal{K} + 1 + \alpha \rho_1 P_{\max})}{\mathcal{I}} P_{\max} \quad (22)$$

$$P_{r,\text{opt}} = \left(1 - \frac{\mathcal{K}(2\mathcal{K} + 2 + (\alpha \rho_1 + \rho_2) P_{\max})}{\mathcal{I}}\right) P_{\max} \quad (23)$$

where $\mathcal{I} \triangleq (\mathcal{K} + 1 + \alpha \rho_1 P_{\max})(\mathcal{K} + 1 + \rho_2 P_{\max}) + (\mathcal{K} + 1 + \alpha \rho_2 P_{\max})(\mathcal{K} + 1 + \rho_1 P_{\max})$. From (21) and (22), we observe that the source associated with the weakest channel, i.e., smaller ρ_i, should transmit more power compared to the source associated with the best channel.

A. The Impact of the IQI Parameter α

From (2), (4), (8) and recalling that $C \triangleq |A|^2 + |B|^2$, we get

$$\alpha \triangleq \frac{C}{D} = \frac{2(1 + g_T^2 g_R^2 + 2 g_T g_R \sin\phi_T \sin\phi_R)}{(1 + g_T^2)(1 + g_R^2)}. \quad (24)$$

Hence,

$$0 \le \frac{2(1 - g_T g_R)^2}{(1 + g_T^2)(1 + g_R^2)} \le \alpha \le \frac{2(1 + g_T g_R)^2}{(1 + g_T^2)(1 + g_R^2)} \le 2.$$

We can now introduce the following insightful corollaries:

Corollary 1: The optimal transmit power at the relay node, $P_{r,\text{opt}}$, is a monotonically decreasing function of α.

Proof: See Appendix I. ■

Corollary 2: Suppose $g_T = g_R = g_{\text{IQI}}$, $\phi_T = \phi_R = \phi$, with $\Delta g_{\text{IQI}} \triangleq \left|1 - g_{\text{IQI}}\right|$ and $\left|\phi\right| < \frac{\pi}{2}$. The optimal transmit power at the relay node, $P_{r,\text{opt}}$, decreases as the IQI at the relay node increases, i.e., as Δg_{IQI} and/or $\left|\phi\right|$ increase.

Proof: See Appendix II. ■

Corollary 1 implies that, in order to maximize the system reliability, the transmit power allocated to the relay node should decrease as the IQI parameter, α, increases, while the total power transmitted from the two source nodes should increase. Corollary 2 claims that, when the relay node has the same TX and RX IQI, the power transmitted from the relay node should decrease if the IQI at the relay node increases.

B. Special Cases

Recall that $C = D = 1$ for the case of perfect I/Q matching. For the case of one-side (TX-only or RX-only) IQI at the relay node, it is easy to show that $C = D = |A|^2 + |B|^2$. Hence, in both special cases, we have $\alpha \triangleq C/D = 1$. Plugging $\alpha = 1$ into (20), we get $\mathcal{K} = \sqrt{(\rho_1 P_{\max} + 1)(\rho_2 P_{\max} + 1)}$. Thus, the optimal amplification factor $\mathtt{G}^2$ in (19) reduces to

$$\mathtt{G}^2_{\text{opt}} = \frac{P_{\max}}{D\left(1 + \sqrt{(\rho_1 P_{\max} + 1)(\rho_2 P_{\max} + 1)}\right)} \quad (25)$$

with $D = 1$ for the ideal case, and $D = |A|^2 + |B|^2$ for the one-side IQI case. The optimal power allocation solution reduces to [4]

$$P_{1,\text{opt}} = \frac{P_{\max}\sqrt{\rho_2 P_{\max}+1}}{2\left(\sqrt{\rho_1 P_{\max}+1}+\sqrt{\rho_2 P_{\max}+1}\right)} \tag{26}$$

$$P_{2,\text{opt}} = \frac{P_{\max}\sqrt{\rho_1 P_{\max}+1}}{2\left(\sqrt{\rho_1 P_{\max}+1}+\sqrt{\rho_2 P_{\max}+1}\right)} \tag{27}$$

$$P_{r,\text{opt}} = \frac{P_{\max}}{2} \tag{28}$$

which is the same for both the one-side IQI case and the ideal hardware case. From (28), we see that, for the two special cases, the relay node and the source nodes should equally share the total transmit power, i.e., $P_{r,\text{opt}} = P_{1,\text{opt}} + P_{2,\text{opt}} = \frac{P_{\max}}{2}$. Note that the optimal solution in (26)-(28), is obtained when $\alpha = 1$. Recall that $P_{r,\text{opt}}$ is a monotonically decreasing function of α. Therefore, when considering joint RX and TX IQI at the relay node, at the optimal point, the power allocated to the relay node should be less than half of the total transmit power if $\alpha > 1$. On the other hand, if $\alpha < 1$, the relay node should transmit with more than half of the total transmit power, in order to maximize the minimum SINR of the two sources.

Plugging (25), (26) and (27) into (12), the received SINR of S_1 and S_2 can be obtained as $\gamma_1 = \gamma_2 = \gamma$, where

$$\gamma = \frac{\rho_1\rho_2 P_{\max}^2}{\kappa\rho_1\rho_2 P_{\max}^2 + 2(1+\kappa)\left(\sqrt{\rho_1 P_{\max}+1}+\sqrt{\rho_2 P_{\max}+1}\right)^2}. \tag{29}$$

In the following, we analyze the OP of two-way relaying, by using the SINR expression in (29), considering one-side only IQI at the relay node with optimal power allocation.

IV. Outage Probability Analysis

Recall that the channel amplitude g_i, $i = 1, 2$, follows a Nakagami-m_i distribution with fading parameters m_i and average powers Ω_i for $i = 1, 2$. Therefore, $\rho_i \triangleq g_i^2$ is a Gamma random variable distributed with shape parameter m_i and scale parameter $\frac{\Omega_i}{m_i}$. The corresponding probability distribution function (PDF) and cumulative distribution function (CDF) for $|h_i|$ and ρ_i can be found in [14, Eq. (2.20) and (2.21)]. The OP at S_i, $i = 1, 2$, is defined as the probability that its instantaneous equivalent SINR, γ_i, falls below a certain threshold γ_{th}, that is,

$$P_{\text{out},i}(\gamma_{\text{th}}) = \Pr\{\gamma_i \le \gamma_{\text{th}}\} \tag{30}$$

where $\Pr\{\cdot\}$ denotes probability. Note that $\gamma_1 = \gamma_2 = \gamma$ for the optimal power allocation. Thus, $P_{\text{out},1}(\gamma_{\text{th}}) = P_{\text{out},2}(\gamma_{\text{th}})$. From (29), the received SINR for both sources can be upper bounded by $\gamma \le \gamma_{\text{upp1}}$, where

$$\gamma_{\text{upp1}} \triangleq \frac{\rho_1\rho_2 P_{\max}^2}{\kappa\rho_1\rho_2 P_{\max}^2 + 2(1+\kappa)\left(\sqrt{\rho_1 P_{\max}}+\sqrt{\rho_2 P_{\max}}\right)^2}$$
$$= \frac{P_{\max}}{\kappa P_{\max} + 2(1+\kappa)\left(\frac{1}{\sqrt{\rho_1}}+\frac{1}{\sqrt{\rho_2}}\right)^2} \tag{31}$$
$$= \frac{X^2}{\kappa X^2 + 2(1+\kappa)} \tag{32}$$

with $X \triangleq \frac{\sqrt{\rho_1\rho_2}P_{\max}}{\sqrt{\rho_1 P_{\max}}+\sqrt{\rho_2 P_{\max}}}$. Based on (32), and utilizing the fact that $\min\left(\sqrt{\rho_1 P_{\max}}, \sqrt{\rho_2 P_{\max}}\right)$ is a tight upper bound of X when $\sqrt{\rho_1 P_{\max}}$ and $\sqrt{\rho_2 P_{\max}}$ grow large, we present the following lower bound on the OP, which becomes exact in the high SNR regime.

Proposition 1: For Nakagami-m fading channels with optimal power allocation, the OP in the presence of one-sided only IQI at the relay node is lower bounded as $P_{\text{out}}(\gamma_{\text{th}}) \ge P_{\text{out,low1}}(\gamma_{\text{th}})$, where

$$P_{\text{out,low1}}(\gamma_{\text{th}}) = 1 - \prod_{i=1}^{2}\left(1 - \frac{\gamma\left(m_i, \frac{m_i}{\Omega_i\tilde{\gamma}}\right)}{\Gamma(m_i)}\right) \tag{33}$$

for $0 \le \gamma_{\text{th}} < \frac{1}{\kappa}$, and $P_{\text{out,low1}}(\gamma_{\text{th}}) = 1$ for $\gamma_{\text{th}} \ge \frac{1}{\kappa}$. Here, $\tilde{\gamma} \triangleq \frac{P_{\max}(1-\kappa\gamma_{\text{th}})}{2(1+\kappa)\gamma_{\text{th}}}$ and $\gamma(s, x) = \int_0^x t^{s-1}\exp(-t)\,dt$ is the lower incomplete Gamma function.

Proof: See Appendix III. ∎

According to the geometric mean-harmonic mean inequality, γ_{upp1} in (32) can be further upper bounded as

$$\gamma_{\text{upp1}} \le \frac{P_{\max} g_1 g_2}{\kappa P_{\max} g_1 g_2 + 8(1+\kappa)}. \tag{34}$$

Now, we provide an alternative lower bound on the OP, which is tight at low and moderate SNRs.

Proposition 2: For Nakagami-m fading channels with optimal power allocation and integer m_2, the OP in the presence of one-sided only IQI at the relay node is lower bounded as $P_{\text{out}}(\gamma_{\text{th}}) \ge P_{\text{out,low2}}(\gamma_{\text{th}})$, where

$$P_{\text{out,low2}}(\gamma_{\text{th}}) = 1 - \frac{2}{\Gamma(m_1)}\left(\frac{m_1}{\Omega_1}\right)^{m_1}\sum_{k=0}^{m_2-1}\frac{1}{k!}\left(\frac{16m_2}{\tilde{\gamma}^2\Omega_2}\right)^k \times\left(\frac{16m_2\Omega_1}{\tilde{\gamma}^2\Omega_2 m_1}\right)^{\frac{m_1-k}{2}} K_{m_1-k}\left(\frac{8}{\tilde{\gamma}}\sqrt{\frac{m_1 m_2}{\Omega_1\Omega_2}}\right) \tag{35}$$

for $0 \le \gamma_{\text{th}} < \frac{1}{\kappa}$, and $P_{\text{out,low2}}(\gamma_{\text{th}}) = 1$ for $\gamma_{\text{th}} \ge \frac{1}{\kappa}$. Here, $K_v(\cdot)$ is the v-th order modified Bessel function of the second kind.

Proof: See Appendix IV. ∎

Note that Proposition 1 applies for any arbitrary fading parameters, whereas Proposition 2 is valid when m_1 and m_2 are positive integers. For the special case of Rayleigh fading, $m_1 = m_2 = 1$, we present the following lower bound on the OP, which remains tight over the entire SNR regime.

Proposition 3: For Rayleigh fading channels with optimal power allocation, the OP in the presence of one-side only IQI at the relay node is lower bounded as $P_{\text{out}}(\gamma_{\text{th}}) \ge P_{\text{out,low3}}(\gamma_{\text{th}})$, where

$$P_{\text{out,low3}}(\gamma_{\text{th}}) = 1 - \sum_{k=0}^{N}\exp\left(-\frac{1}{\tilde{\gamma}\Omega_1}\left(1+\frac{1}{(k+1)\Delta t}\right)^2\right) \times\left(\exp\left(-\frac{(k\Delta t+1)^2}{\tilde{\gamma}\Omega_2}\right) - \exp\left(-\frac{((k+1)\Delta t+1)^2}{\tilde{\gamma}\Omega_2}\right)\right) - \exp\left(-\frac{1}{\tilde{\gamma}\Omega_1} - \frac{((N+1)\Delta t+1)^2}{\tilde{\gamma}\Omega_2}\right) \tag{36}$$

for $0 \le \gamma_{\text{th}} < \frac{1}{\kappa}$, and $P_{\text{out,low3}}(\gamma_{\text{th}}) = 1$ for $\gamma_{\text{th}} \ge \frac{1}{\kappa}$. Here, N is an arbitrary positive integer and the interval Δt is an arbitrary positive value.

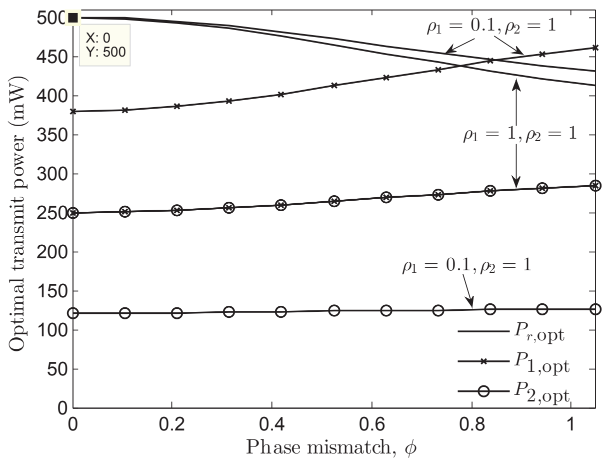

Fig. 2. Optimal transmit powers $P_{1,\text{opt}}$, $P_{2,\text{opt}}$ and $P_{r,\text{opt}}$ vs. the phase mismatch parameter ϕ. The maximum total transmit power is $P_{\max} = 40$mW.

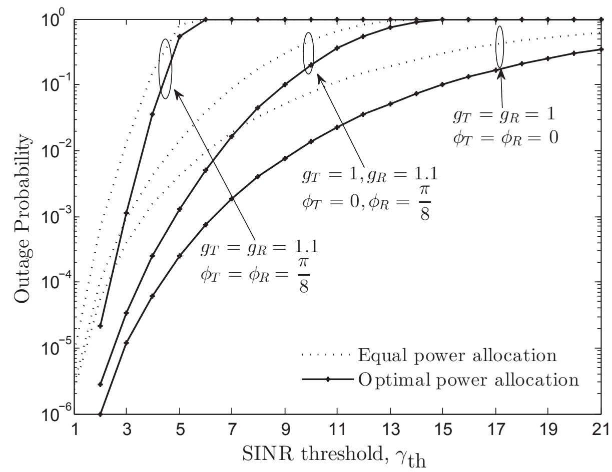

Fig. 3. The maximum outage probability vs. SINR threshold γ_{th} for different IQI parameters. The maximum transmit power is $P_{\max} = 25$dBm. The channel fading parameters are $m_1 = m_2 = 5$, $\Omega_1 = 0.5$ and $\Omega_2 = 1$.

Proof: See Appendix V. ■

The choice of N and Δt affects the tightness of the lower bound. In general, a larger N combined with a smaller Δt will provide a tighter lower bound.

From Propositions 1, 2 and 3, we see that, due to the effect of IQI, the OP is always 1 if γ_{th} is above the inverse of the joint image-leakage ratio. This implies that, for high levels of IQI, the system is always in outage, which cannot be avoided by simply hardening the channel conditions or transmitting more power. This observation is in line with [15], [16].

V. Numerical Results

In this section, we present a set of numerical results to evaluate the performance of the power allocation scheme and to verify our analytical results. The noise power is assumed to be 1mW. Figure 2 shows the optimal power values in (21), (22) and (23) as functions of the phase mismatch parameter, ϕ, for two different channel realizations, i.e., $\rho_1 = \rho_2 = 1$ and $\rho_1 = 0.1, \rho_2 = 1$. We consider a symmetric IQI case with $\phi_T = \phi_R = \phi$ and $g_T = g_R = 1$. In agreement with Corollary 2, the optimal transmit power at the relay node, $P_{r,\text{opt}}$, decreases as the phase imbalance, ϕ, increases. We also observe that for the considered asymmetric channel case, the source associated with the weaker link transmits with a higher power, which increases as ϕ increases. On the other hand, the optimal transmit power at the source associated with the stronger link, remains unaffected by the phase imbalance. Moreover, as anticipated, for the special case of perfect I/Q matching, i.e., when $\phi_T = \phi_R = 0$ and $g_T = g_R = 1$, the optimal value for $P_{r,\text{opt}}$ is always $P_{\max}/2$, which is independent of the channel conditions.

Figure 3 demonstrates the maximum OP of the two sources, i.e., $\max\left(P_{\text{out},1}(\gamma_{\text{th}}), P_{\text{out},2}(\gamma_{\text{th}})\right)$, versus the target SINR γ_{th}. The proposed optimal power allocation scheme is compared with the equal power allocation scheme, where $P_1 = P_2 = P_r = P_{\max}/3$. We consider two IQI cases: the joint IQI case with $g_T = g_R = 1.1$, $\phi_T = \phi_R = \frac{\pi}{8}$; and the RX-only IQI case with $g_R = 1.1$ and $\phi_R = \frac{\pi}{8}$. The corresponding values of the joint image-leakage ratio, κ, are 0.15 and 0.04 respectively. Recall that $g_T = g_R = 1$, $\phi_T = \phi_R = 0$ represents the perfect I/Q matching case with $\kappa = 0$. By increasing κ, the performance loss compared to the case with perfect I/Q matching increases substantially for both power allocation schemes. For the considered IQI cases, the OP becomes equal to 1 once the SINR threshold, γ_{th}, reaches to the SINR ceiling, i.e., $\frac{1}{\kappa}$. This implies that the system is in full outage due to the effect of IQI, which is in fundamental contrast to the perfect I/Q matching case where the SINR ceiling effect does not occur. We also observe that, at low values of γ_{th}, i.e., when $\gamma_{\text{th}} \ll \frac{1}{\kappa}$, power allocation is important for reducing the IQI effects, thereby improving the outage performance.

Figure 4 investigates the analytical lower bounds derived in Propositions 1 and 2 for the OP versus $P_{\max}$ for different fading parameters m. As anticipated, we see that the OP decreases as m increases, since the channel condition becomes better when m becomes large. Moreover, $P_{\text{out,low1}}(\gamma_{\text{th}})$ matches well with the numerical results for very large $P_{\max}$ and $P_{\text{out,low2}}(\gamma_{\text{th}})$ is tight for small and moderate $P_{\max}$. Generally speaking, in the performance evaluation, the maximum of these two lower bounds can be selected to predict the exact OP with a better accuracy. In Fig. 5, we examine $P_{\text{out,low3}}(\gamma_{\text{th}})$ derived in Proposition 3 for the Rayleigh fading case. As mentioned before, a larger N combined with a smaller Δt will provide a tighter lower bound. Yet, we observe that the improvement brought by further increasing N beyond 10 becomes negligible. In addition, compared to the equal power allocation scheme, we see that the proposed scheme can significantly improve the maximum OP, thus improving the reliability of both sources, especially when the total power budget $P_{\max}$ is large.

VI. Conclusions

We analyzed the performance of a dual-hop two-way AF relaying system, where the relay node suffers from both TX and RX IQI. An instantaneous power allocation scheme was proposed to maximize the minimum SINR of the two sources under a total transmit power constraint. Moreover, tractable

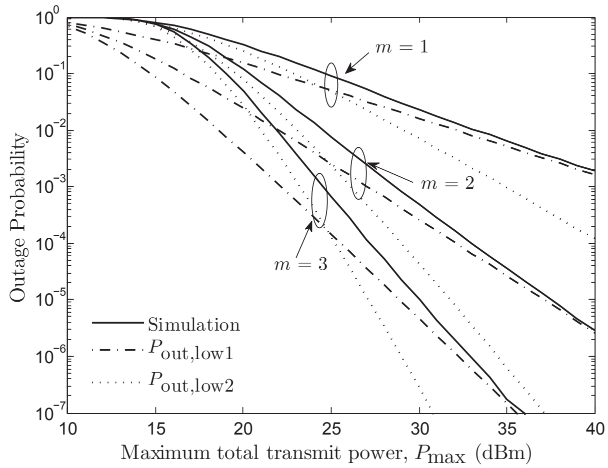

Fig. 4. Outage probability vs. P_{max}. The channel fading parameters are $m_1 = m_2 = m$, $\Omega_1 = \Omega_2 = 0.5$. The SINR threshold $\gamma_{\text{th}} = 2$. The IQI parameters are $g_T = 1$, $g_R = 1.1$, $\phi_T = 0$ and $\phi_R = \pi/30$.

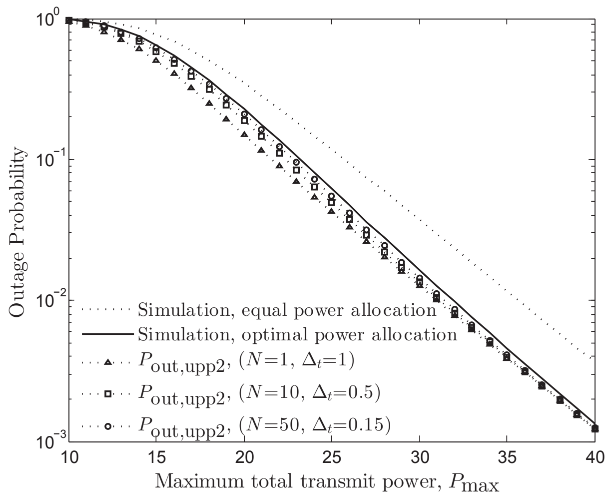

Fig. 5. Outage probability vs. P_{max}. The channel fading parameters are $m_1 = m_2 = 1$, $\Omega_1 = 0.5$ and $\Omega_2 = 1$. The SINR threshold $\gamma_{\text{th}} = 2$. The IQI parameters are $g_T = 1$, $g_R = 1.1$, $\phi_T = 0$ and $\phi_R = \pi/30$.

lower bounds have been derived for the outage probability over Nakagami-m fading channels. Our theoretical analysis indicated that, for high levels of IQI, the system is always in outage, which cannot be avoided by simply hardening the channel conditions. Compared to the equal power allocation scheme, it was also shown that the proposed power allocation scheme can significantly improve the outage performance, thus reducing the IQI effects, especially when the total power budget is large.

Appendix I
Proof of Corollary 1

From (23), we get $P_{r,\text{opt}} = P_{\max}\frac{x(\alpha)}{y(\alpha)}$, where

$$x(\alpha) \triangleq 2\left(\left(\mathcal{I}_1 + \mathcal{I}_2\right)\alpha + \left(\mathcal{I}_2 + 1\right)\left(\mathcal{K} + 1\right)\right)$$

$$y(\alpha) \triangleq 2\left(\left(\mathcal{I}_1 + \mathcal{I}_2\right)\alpha + \left(\mathcal{K} + 1\right)^2 + \mathcal{I}_2\mathcal{K}\left(\alpha + 1\right) + \mathcal{I}_2\right)$$

with $\mathcal{I}_1 \triangleq \rho_1\rho_2 P_{\max}^2$ and $\mathcal{I}_2 \triangleq \frac{\rho_1+\rho_2}{2}P_{\max}$. It is sufficient to show that $f(\alpha) \triangleq \frac{\partial x(\alpha)}{\partial \alpha}y(\alpha) - x(\alpha)\frac{\partial y(\alpha)}{\partial \alpha} < 0$ for $0 \le \alpha \le 2$. After some basic algebra, we get

$$f(\alpha) = 2\mathcal{K}\left(\mathcal{I}_1 - 3\mathcal{I}_2^2 - \mathcal{I}_2 - \mathcal{I}_1\mathcal{I}_2\right) - \mathcal{I}_3$$

where $\mathcal{I}_3 = \frac{2}{\mathcal{K}}\left(\mathcal{I}_1 + \mathcal{I}_2\right)\left(1 + \alpha\mathcal{I}_2\right)\left(1 + \mathcal{I}_2 + \alpha\left(\mathcal{I}_1 + \mathcal{I}_2\right)\right) + 4\mathcal{I}_2\mathcal{K}^2\left(\mathcal{I}_2 + 1\right) > 0$. Utilizing the fact that the geometric mean is smaller or equal to the arithmetic mean, we have $\mathcal{I}_1 \le \mathcal{I}_2^2$. Hence, $f(\alpha) < 0$, i.e., $P_{r,\text{opt}}$ decreases as α increases.

Appendix II
Proof of Corollary 2

Substituting $g_T = g_R = g_{\text{IQI}}$ and $\phi_T = \phi_R = \phi$ into (24), we get

$$\alpha = 2 + \frac{4g_{\text{IQI}}^2\left(\left(\sin\phi\right)^2 - 1\right)}{\left(1 + g_{\text{IQI}}^2\right)^2}. \tag{37}$$

Hence, α increases as $\left|\phi\right|$ increases for $\left|\phi\right| < \frac{\pi}{2}$. The first derivative of α with respect to g_{IQI} can be derived as

$$\frac{\partial \alpha}{\partial g_{\text{IQI}}} = \frac{8g_{\text{IQI}}\left(\left(\sin\phi\right)^2 - 1\right)\left(1 - g^2\right)}{\left(1 + g_{\text{IQI}}^2\right)^3} \begin{cases} \le 0, & g_{\text{IQI}} \ge 1, \\ \ge 0, & 0 < g_{\text{IQI}} \le 1. \end{cases} \tag{38}$$

Thus, if $g_{\text{IQI}} \ge 1$, α increases as g_{IQI} increases; otherwise, if $0 < g_{\text{IQI}} \le 1$, then α increases as g_{IQI} decreases. Therefore, α increases as $\Delta g_{\text{IQI}} \triangleq \left|1 - g_{\text{IQI}}\right|$ increases. Combined with Corollary 1, the statement in Corollary 2 is proved.

Appendix III
Proof of Proposition 1

Note that $X \le \min\left(\sqrt{\rho_1 P_{\max}}, \sqrt{\rho_2 P_{\max}}\right)$. Hence,

$$\gamma_{\text{upp1}} \le \frac{\left(\min\left(\sqrt{\rho_1 P_{\max}}, \sqrt{\rho_2 P_{\max}}\right)\right)^2}{\kappa\left(\min\left(\sqrt{\rho_1 P_{\max}}, \sqrt{\rho_2 P_{\max}}\right)\right)^2 + 2\left(1 + \kappa\right)}. \tag{39}$$

Therefore, $P_{\text{out}}(\gamma_{\text{th}})$ can be lower bounded by $P_{\text{out}}(\gamma_{\text{th}}) \ge P_{\text{out,low1}}(\gamma_{\text{th}})$, where

$$\begin{aligned} &P_{\text{out,low1}}(\gamma_{\text{th}}) \\ &= \Pr\left\{\frac{\left(\min\left(\sqrt{\rho_1 P_{\max}}, \sqrt{\rho_2 P_{\max}}\right)\right)^2}{\kappa\left(\min\left(\sqrt{\rho_1 P_{\max}}, \sqrt{\rho_2 P_{\max}}\right)\right)^2 + 2\left(1 + \kappa\right)} \le \gamma_{\text{th}}\right\} \\ &= \begin{cases} 1, & \gamma_{\text{th}} \ge \frac{1}{\kappa}, \\ F_{\min\left(\sqrt{\rho_1 P_{\max}}, \sqrt{\rho_2 P_{\max}}\right)}\left(\sqrt{\frac{2(1+\kappa)\gamma_{\text{th}}}{1-\kappa\gamma_{\text{th}}}}\right), & 0 \le \gamma_{\text{th}} < \frac{1}{\kappa} \end{cases} \end{aligned} \tag{40}$$

where

$$\begin{aligned} &F_{\min\left(\sqrt{\rho_1 P_{\max}}, \sqrt{\rho_2 P_{\max}}\right)}\left(\sqrt{\frac{2\left(1+\kappa\right)\gamma_{\text{th}}}{1-\kappa\gamma_{\text{th}}}}\right) \\ &\triangleq \Pr\left\{\min\left(\sqrt{\rho_1 P_{\max}}, \sqrt{\rho_2 P_{\max}}\right) \le \sqrt{\frac{2\left(1+\kappa\right)\gamma_{\text{th}}}{1-\kappa\gamma_{\text{th}}}}\right\} \\ &\overset{(a)}{=} 1 - \Pr\left\{\rho_1 > \frac{2\left(1+\kappa\right)\gamma_{\text{th}}}{P_{\max}\left(1-\kappa\gamma_{\text{th}}\right)}\right\}\Pr\left\{\rho_2 > \frac{2\left(1+\kappa\right)\gamma_{\text{th}}}{P_{\max}\left(1-\kappa\gamma_{\text{th}}\right)}\right\} \\ &= 1 - \prod_{i=1}^{2}\left(1 - \frac{\gamma\left(m_i, \frac{m_i}{\Omega_i\tilde{\gamma}}\right)}{\Gamma(m_i)}\right). \end{aligned} \tag{41}$$

Here, (a) follows from the fact that ρ_1 and ρ_2 are independent of each other. The desired result is obtained by substituting (41) into (40).

APPENDIX IV
PROOF OF PROPOSITION 2

Let $p_{g_i}(x)$ and $F_{g_i}(x)$ denote the PDF and CDF of g_i, respectively. From (34), $P_{\text{out}}(\gamma_{\text{th}})$ can be lower bounded by $P_{\text{out}}(\gamma_{\text{th}}) \geq P_{\text{out,low2}}(\gamma_{\text{th}})$, where

$$P_{\text{out,low2}}(\gamma_{\text{th}}) = \Pr\left\{\frac{g_1 g_2 P_{\max}}{\kappa g_1 g_2 P_{\max} + 8(1+\kappa)} \leq \gamma_{\text{th}}\right\} = \begin{cases} 1, & \gamma_{\text{th}} \geq \frac{1}{\kappa}, \\ \Pr\left\{g_1 g_2 \leq \frac{4}{\tilde{\gamma}}\right\}, & 0 \leq \gamma_{\text{th}} < \frac{1}{\kappa} \end{cases} \quad (42)$$

with

$$\Pr\left\{g_1 g_2 \leq \frac{4}{\tilde{\gamma}}\right\} = \int_0^\infty p_{g_1}(x) F_{g_2}\left(\frac{4}{\tilde{\gamma}x}\right) dx \quad (43)$$

$$= 1 - \frac{2}{\Gamma(m_1)}\left(\frac{m_1}{\Omega_1}\right)^{m_1} \sum_{k=0}^{m_2-1} \frac{1}{k!}\left(\frac{m_2}{\Omega_2}\right)^k \left(\frac{4}{\tilde{\gamma}}\right)^{2k} J_k \quad (44)$$

where from (43) to (44) we have used the binomial expansion for integer m_2. Also,

$$J_k \triangleq \int_0^\infty x^{2m_1-2k-1} \exp\left(-\frac{m_1}{\Omega_1}x^2 - \frac{16 m_2}{\tilde{\gamma}^2 \Omega_2}\frac{1}{x^2}\right) dx \quad (45)$$

$$= \left(\frac{16 m_2 \Omega_1}{\tilde{\gamma}^2 \Omega_2 m_1}\right)^{\frac{m_1-k}{2}} K_{m_1-k}\left(\frac{8}{\tilde{\gamma}}\sqrt{\frac{m_1 m_2}{\Omega_1 \Omega_2}}\right). \quad (46)$$

Here, we have used [17, Eq. (3.478.4)] to evaluate the integral in (45). By substituting (46) into (44) and combining it with (42), the result in (35) is obtained.

APPENDIX V
PROOF OF PROPOSITION 3

From (31), $P_{\text{out}}(\gamma_{\text{th}})$ can be lower bounded by

$$P_{\text{out}}(\gamma_{\text{th}}) \geq \Pr\left\{\frac{P_{\max}}{\kappa P_{\max} + 2(1+\kappa)\left(\frac{1}{g_1}+\frac{1}{g_2}\right)^2} \leq \gamma_{\text{th}}\right\} = \begin{cases} 1, & \gamma_{\text{th}} \geq \frac{1}{\kappa}, \\ \Pr\left\{\frac{1}{g_1}+\frac{1}{g_2} \geq \sqrt{\tilde{\gamma}}\right\}, & 0 \leq \gamma_{\text{th}} < \frac{1}{\kappa} \end{cases} \quad (47)$$

with

$$\Pr\left\{\frac{1}{g_1}+\frac{1}{g_2} \geq \sqrt{\tilde{\gamma}}\right\} = 1 - \frac{2}{\tilde{\gamma}\Omega_2}\mathcal{I}_4 \quad (48)$$

where $\mathcal{I}_4 \triangleq \tilde{\gamma}\int_{\sqrt{\frac{1}{\tilde{\gamma}}}}^\infty x \exp\left(-\frac{1}{\Omega_1}\frac{x^2}{(\sqrt{\tilde{\gamma}}x-1)^2} - \frac{1}{\Omega_2}x^2\right) dx$. By making the change of variables $y \to \sqrt{\tilde{\gamma}}x$, we get

$$\mathcal{I}_4 = \int_1^\infty y \exp\left(-\frac{1}{\tilde{\gamma}\Omega_2}y^2\right) f(y)\, dy = \sum_{k=0}^{N} \int_{k\Delta t+1}^{(k+1)\Delta t+1} y \exp\left(-\frac{1}{\tilde{\gamma}\Omega_2}y^2\right) f(y)\, dy + \int_{(N+1)\Delta t+1}^{\infty} y \exp\left(-\frac{1}{\tilde{\gamma}\Omega_2}y^2\right) f(y)\, dy$$

where $f(y) \triangleq \exp\left(-\frac{1}{\tilde{\gamma}\Omega_1}\left(1+\frac{1}{y-1}\right)^2\right)$. Note that $f(y)$ is an increasing function of y for $y > 1$. Hence,

$$I_4 \leq \sum_{k=0}^{N} \exp\left(-\frac{1}{\tilde{\gamma}\Omega_1}\left(1+\frac{1}{(k+1)\Delta t}\right)^2\right) \times \int_{k\Delta t+1}^{(k+1)\Delta t+1} y \exp\left(-\frac{y^2}{\tilde{\gamma}\Omega_2}\right) dy + \exp\left(-\frac{1}{\tilde{\gamma}\Omega_1}\right)\int_{(N+1)\Delta t+1}^\infty y \exp\left(-\frac{y^2}{\tilde{\gamma}\Omega_2}\right) dy. \quad (49)$$

By evaluating the integrals in (49) with the aid of [17, Eq. (3.381.9)], then substituting the result into (48) and combining with (47), we can readily obtain (36).

REFERENCES

[1] C. Hoymann, W. Chen, J. Montojo, A. Golitschek, C. Koutsimanis, and X. Shen, "Relaying operation in 3GPP LTE: Challenges and solutions," *IEEE Commun. Mag.*, vol. 50, no. 2, pp. 156–162, June 2012.

[2] B. Rankov and A. Wittneben, "Spectral efficient protocols for half-duplex fading relay channels," *IEEE J. Sel. Areas Commun.*, vol. 25, no. 2, pp. 379–389, Feb. 2007.

[3] R. H. Y. Louie, Y. Li, and B. Vucetic, "Practical physical layer network coding for two-way relay channels: Performance analysis and comparison," *IEEE Trans. Wireless Commun.*, vol. 9, no. 2, pp. 764–777, Feb. 2010.

[4] S. Talwar, Y. Jing, and S. Shahbazpanahi, "Joint relay selection and power allocation for two-way relay networks," *IEEE Signal Process. Lett.*, vol. 18, no. 2, pp. 91–94, Feb. 2011.

[5] V. Havary-Nassab, S. Shahbazpanahi, and A. Grami, "Optimal distributed beamforming for two-way relay networks," *IEEE Trans. Signal Process.*, vol. 58, no. 3, pp. 1238–1250, Mar. 2010.

[6] T. Schenk, *RF Imperfections in High-Rate Wireless Systems: Impact and Digital Compensation*. Springer Netherlands, 2008.

[7] J. Qi, S. Aïssa, and M.-S. Alouini, "Analysis and compensation of I/Q imbalance in amplify-and-forward cooperative systems," in *Proc. IEEE Wireless Commun. Netw. Conf. (WCNC)*, Apr. 2012, pp. 215–220.

[8] M. Mokhtar, A. Gomaa, and N. Al-Dhahir, "OFDM AF relaying under I/Q imbalance: Performance analysis and baseband compensation," *IEEE Trans. Commun.*, vol. 61, no. 4, pp. 1304–1313, Apr. 2013.

[9] J. Li, M. Matthaiou, and T. Svensson, "I/Q imbalance in AF dual-hop relaying: Performance analysis in Nakagami-m fading," *in press IEEE Trans. Commun.*, pp. 1–12, 2014.

[10] J. Qi, S. Aïssa, and M.-S. Alouini, "Impact of I/Q imbalance on the performance of two-way CSI-assisted AF relaying," in *Proc. IEEE Wireless Commun. Netw. Conf. (WCNC)*, Apr. 2013, pp. 2507–2512.

[11] M. Valkama, M. Renfors, and V. Koivunen, "Advanced methods for I/Q imbalance compensation in communication receivers," *IEEE Trans. Signal Process.*, vol. 49, no. 10, pp. 2335–2344, Oct 2001.

[12] J. Qi and S. Aïssa, "Analysis and compensation of I/Q imbalance in MIMO transmit-receive diversity systems," *IEEE Trans. Commun.*, vol. 58, no. 5, pp. 1546–1556, May 2010.

[13] Ö. Özdemir, R. Hamila, and N. Al-Dhahir, "I/Q imbalance in multiple beamforming OFDM transceivers: SINR analysis and digital baseband compensation," *IEEE Trans. Commun.*, vol. 61, no. 5, pp. 1914–1925, May 2013.

[14] M. K. Simon and M.-S. Alouini, *Digital Communication over Fading Channels*, 2nd ed. John Wiley & Sons, 2005.

[15] M. Matthaiou, A. Papadogiannis, E. Björnson, and M. Debbah, "Two-way relaying under the presence of relay transceiver hardware impairments," *IEEE Commun. Lett.*, vol. 17, no. 6, pp. 1136–1139, June 2013.

[16] E. Björnson, M. Matthaiou, and M. Debbah, "A new look at dual-hop relaying: Performance limits with hardware impairments," *IEEE Trans. Commun.*, vol. 61, no. 11, pp. 4512–4525, Nov. 2013.

[17] I. S. Gradshteyn and I. M. Ryzhik, *Table of Integrals, Series, and Products*, 7th ed. Academic Press, 2007.